Electrical Manipulation of Supported Lipid Membranes by Embedded Electrodes

Bryan L. Jackson,[†] Jeffrey A. Nye,[‡] and Jay T. Groves*[,†,§]

Departments of Chemistry and Chemical Engineering, University of California, Berkeley, California 94720, and Physical Bioscience and Material Science Divisions, Lawrence Berkeley National Laboratory, Berkeley, California 94720

Received January 7, 2008. Revised Manuscript Received March 6, 2008

Alkanethiol modified gold electrodes patterned over a silica surface provided a dual hydrophobic/hydrophilic surface suitable for phospholipid monolayer and bilayer formation over the alkylated gold and glass surfaces, respectively. The phospholipid monolayer and bilayer were connected, allowing free diffusion of lipids within both leaflets of the glass-supported bilayer over the alkanethiol/gold-to-glass interface. Application of large alternating current fields to these electrodes irreversibly switched the gold electrodes to diffusion barriers. Enclosure of the electrode devices within protein barriers revealed a resting state surface potential driven reorganization of the charged fluorescent probes. Application of lower magnitude direct current fields resulted in electrophoretic redistribution of the membrane probes and electro-osmotic reorganization of membrane associated proteins.

Introduction

When properly prepared, phospholipids coupled to a solid support retain the two-dimensional fluidity necessary for dynamic rearrangement of signaling molecules and are readily interfaced with living cells.[1–3] Living cells are dynamic in nature and routinely drive membrane components toward lower entropic states with great precision.[4,5] While recent studies have demonstrated comparable spatial control of lipid membranes,[6–9] similar temporal control has yet to be demonstrated. Thus, dynamic surfaces that can change the concentration profiles of membrane associated components in space and time are highly desirable. Prior work has outlined a technique to impose and then remove barriers to lipid diffusion by mechanically scoring the underlying substrate.[10] Additionally, external electric fields offer the ability to reorganize charged lipid components[11] and membrane associated proteins[12] according to the interplay of electrophoretic and electro-osmotic forces.[13] However, reorganization in this manner provides only a one-dimensional redistribution of membrane associated molecules. Two-dimensional control of these concentration profiles would provide a substantial improvement in supported membrane technology.

Electrodes embedded within a supported lipid membrane, introduced herein, offer the unique opportunity to modulate charged lipid probes and membrane associated protein distributions at time scales similar to those of live cells (on the order of minutes). Particularly, these electrodes offer the ability to irreversibly gate lipid diffusion and to control the concentration profiles of fluorescent lipid probes and proteins in two dimensions. Gating lipid diffusion requires a short pulse at high alternating current (AC) fields to electrochemically remove alkanethiol monolayers, while lower magnitude direct current (DC) fields cause lipid probes and proteins to reorganize according to electrophoretic and electro-osmotic forces, respectively.

Experimental Section

Electrode Patterning. Electrode patterning was accomplished by traditional lift-off lithography. Briefly, 4 in. silica wafers were coated with hexamethyldisilazane (HMDS) by gas phase reaction for 10 min to promote photoresist adhesion. Next, s1805 photoresist (Rohm and Haas Electronic Materials, Malborough, MA) was spun onto wafers at 4500 rpm and then baked at 90 °C for 10 min. Resist was exposed at 27.3 mJ/cm^2 with a Quintel Corp. (Morgan Hill, CA) Q4000 mask aligner. Wafers were then developed in a 1:1 mixture of MicroDev to deionized water for 35 s. Substrates were rinsed six times in deionized water and then dried under a nitrogen stream. Wafers were coated with 5 nm of chromium (99.999%) followed by 30 nm of gold (99.999%) by thermal evaporation. Residual resist and the associated metal layer were removed in 50 °C acetone followed by 30 min sonication in fresh acetone. Substrates were piranha cleaned directly before the next step.

Aluminum, Alignment, and Protein Patterning. Protein patterns were produced according to the aluminum lift-off protocol described previously,[7] except where noted. Piranha cleaned electrode patterned substrates were coated with a thin aluminum film by sputtering. Photoresist (s1805) was spun, exposed, and developed without deviation from established protocols. The electrode patterns and the next mask were aligned with coarse (50 μm) and then fine (2 μm) alignment marks. Aluminum etching, resist removal, and fibronectin binding were also processed without deviation from described protocols. Unlike in the previous protocol, aluminum was dissolved in 100 mM sodium bicarbonate solution (pH 12) for 20 min followed by a 30 s submersion in 100 mM hydrochloric acid solution.

* To whom correspondence should be addressed. E-mail: jtgroves@lbl.gov.
[†] Department of Chemistry, University of California.
[‡] Department of Chemical Engineering, University of California.
[§] Lawrence Berkeley National Laboratory.

(1) Groves, J. T.; Mahal, L. K.; Bertozzi, C. R. *Langmuir* **2001**, *17*, 5129–5133.
(2) Lee, K. H.; Holdorf, A. D.; Dustin, M. L.; Chan, A. C.; Allen, P. M.; Shaw, A. S. *Science* **2002**, *295*, 1539–1542.
(3) Wu, M.; Holowka, D.; Craighead, H. G.; Baird, B. *Proc. Natl. Acad. Sci. U.S.A.* **2004**, *101*, 13798–13803.
(4) Grakoui, A.; Bromley, S. K.; Sumen, C.; Davis, M. M.; Shaw, A. S.; Allen, P. M.; Dustin, M. L. *Science* **1999**, *285*, 221–227.
(5) Mossman, K. D.; Campi, G.; Groves, J. T.; Dustin, M. L. *Science* **2005**, *310*, 1191–1193.
(6) Jackson, B. L.; Groves, J. T. *J. Am. Chem. Soc.* **2004**, *126*, 13878–13879.
(7) Jackson, B. L.; Groves, J. T. *Langmuir* **2007**, *23*, 2052–2057.
(8) Lenhert, S.; Sun, P.; Wang, Y. H.; Fuchs, H.; Mirkin, C. A. *Small* **2007**, *3*, 71–75.
(9) Shi, J.; Chen, J.; Cremer, P. S. *J. Am. Chem. Soc.* **2008**, *130*, 2718–2719.
(10) Cremer, P. S.; Groves, J. T.; Kung, L. A.; Boxer, S. G. *Langmuir* **1999**, *15*, 3893–3896.
(11) Groves, J. T.; Boxer, S. G.; McConnell, H. M. *Proc. Natl. Acad. Sci. U.S.A.* **1998**, *94*, 13390–13395.
(12) Grogan, M. J.; Kaizuka, Y.; Conrad, R. M.; Groves, J. T.; Bertozzi, C. R. *J. Am. Chem. Soc.* **2005**, *127*, 14383–14387.
(13) Yoshina-Ishii, C.; Boxer, S. G. *Langmuir* **2006**, *22*, 2384–2391.

10.1021/la800040w CCC: $40.75
Published on Web 05/21/2008

Monolayer Formation. Following aluminum removal for substrates with protein patterns, or piranha cleaning for substrates without protein structures, substrates were immersed in a 3 mM solution of 1-octadecanethiol (Sigma-Aldrich, St. Louis, MO) in hexane for at least 13 h and up to 4 weeks. Immediately before use, substrates were rinsed successively in hexane, acetone, 2-propanol, dried under a N_2 stream, and then immersed in deionized water 3 times and dried again. Interestingly, prolonged storage of piranha cleaned glass in hexane did not negatively affect the propensity of vesicles to rupture and form fluid supported bilayers over glass. Etched coverslips stored in hexane for 4 weeks readily formed fluid bilayers, while approximately one day in water or ambient atmosphere rendered etched glass surfaces incapable of supported bilayer formation.

Bilayer Deposition, Protein Binding, and Electric Contact. The experimental area was enclosed within a ~2 mm diameter well made from hot glue. The hybrid supported bilayer/monolayer was deposited over the surface by 1 min incubation in 1 mg/mL small unilamellar vesicle (SUV) solution, egg-PC (Avanti Polar Lipids, Alabaster, AL) doped with 1 mol % Texas Red-DHPE (Invitrogen, Carlsbad, CA), in a 5 mM TRIS, 100 mM sodium chloride, pH 7.4 solution. The remaining SUV solution was washed in >100× excess of deionized water. For protein experiments, small unilamellar vesicles (SUVs) consisted of 5% 1,2-dioleoyl-*sn*-glycero-3-[(*N*-(5-amino-1-carboxypentyl)iminodiacetic acid)succinyl] (DOGS-NTA) and 0.5% TR-DHPE in 1,2-dioleoyl-*sn*-glycero-3-phosphocholine (DOPC). Histidine-10 modified green fluorescent protein was coupled to the membrane at a concentration of 2 mM for 20 min and then washed with >100× excess of deionized water. A 0.0005 in. diameter platinum wire (A-M Systems, Carlsborg, WA) was connected to the gold electrodes by indium (Sigma-Aldrich, St. Louis, MO) stamping. The platinum wire was then connected to an AFG3102 Tektronix signal generator (Beaverton, OR).

Results

Diffusion Across the Interface. When alkanethiol modified gold electrodes patterned over glass were exposed to an aqueous suspension of vesicles, a bilayer composed of phospholipids formed over the silica surface and was juxtaposed with a hybrid bilayer, consisting of a fluid phospholipid monolayer over an immobile alkanethiol monolayer[14,15] (Figure 1A). Although fluorophores were present over the gold surfaces, these portions remained dark for two reasons: quenching of the fluorescent probes by the metal layer[16–18] and disruption of the light path (excitation and emission) on the inverted microscope. A unique feature of the hybrid lipid monolayer/bilayer configuration presented here versus previously published systems[19,20] was that the phospholipid monolayer and bilayer were connected and could freely diffuse over the gold electrodes as demonstrated by fluorescence recovery after photobleaching (FRAP) of the fluorescent lipid probe, Texas Red-DHPE (Figure 1B and C). When the thiol monolayer was absent, there was no diffusion over the gold film (Figure 1D and E).

Surprisingly, the fluorescence within the inner electrode (completely surrounded by the gold/alkanethiol film) routinely recovered to 90–95% of the original intensity within 70 min. This was unexpected because only a phospholipid monolayer

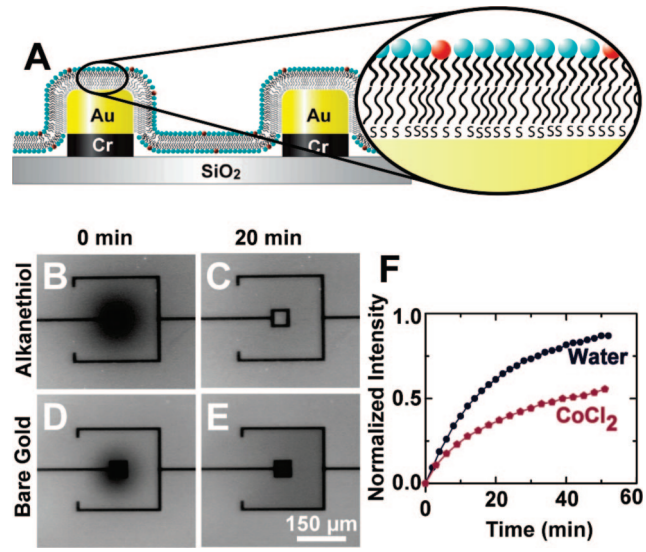

Figure 1. (A) Schematic of the electrode system. The bilayer-to-monolayer interface was not characterized. (B−E) Fluorescence images directly following and 20 min after photobleaching of Texas Red-DHPE on substrates with (B and C) and without (D and E) a C_{18}-thiol monolayer over the gold surfaces. Membranes flowed freely over the alkanethiol derivatized gold surfaces but not over bare gold. (F) Fluorescence recovery in the absence and presence of 50 mM cobalt(II) chloride which quenches upper leaflet fluorescence. Traces were normalized to unbleached regions in each sample (i.e., unit intensity represented complete recovery). The observed recovery trace in the presence of cobalt(II) chloride indicated that the lower leaflet of the glass supported bilayer diffused over the alkylated gold surface.

can diffuse over the alkanethiol surface. This finding implied that the lower and upper leaflets were mixing (a trait not depicted in Figure 1A). This hypothesis was confirmed by adding 50 mM cobalt(II) chloride to the system to quench the upper membrane's fluorescence.[21,22] Fluorescence analysis before and after $CoCl_2$ addition indicated that nearly 80% of the fluorescence intensity from Texas Red was due to the upper leaflet. FRAP analysis confirmed that the lower leaflet recovered over the gold electrodes but at a slower rate than the upper leaflet (Figure 1F). This observation could be explained by the propensity for lipids to flip-flop at defects located at membrane interfaces.[22–24] The dependence of recovery on the limited defect portion at the interface between the lipid monolayer and bilayer explained the slowed recovery rate of the proximal leaflet compared to the distal.

Irreversible Lipid Gating. The alkylated gold surface provided a means to irreversibly modulate membrane diffusion by application of large magnitude electric fields. However, electric fields can cause electrophoretic reorganization of the charged probe used in this study.[11,25] To mitigate this effect, an AFG3102 Tektronix signal generator [Beaverton, OR] was used to provide haversine waveforms, unipolar sine waves, with amplitudes between 0.1 and 6 V at 1 kHz. Additionally, high frequency fields allowed access to higher voltages than otherwise possible due to the electrochemical gas evolution observed at high fields and low frequencies.[26,27] This bubble formation proved detrimental to supported bilayers. Effective gating of membrane

(14) Plant, A. L. *Langmuir* **1999**, *15*, 5128–5135.
(15) Plant, A. L.; Gueguetchkeri, M.; Yap, W. *Biophys. J.* **1994**, *67*, 1126–1133.
(16) Dulkeith, E.; Morteani, A. C.; Niedereichholz, T.; Klar, T. A.; Feldmann, J.; Levi, S. A.; van Veggel, F. C.; Reinhoudt, D. N.; Moller, M.; Gittins, D. I. *Phys. Rev. Lett.* **2002**, *89*, 203002.
(17) Weber, W. H.; Eagen, C. F. *Opt. Lett.* **1979**, *4*, 236.
(18) Weitz, D. A.; Garoff, S.; Gersten, J. I.; Nitzan, A. *J. Chem. Phys.* **1983**, *78*, 5324–5338.
(19) Howland, M. C.; Sapuri-Butti, A. R.; Dixit, S. S.; Dattelbaum, A. M.; Shreve, A. P.; Parikh, A. N. *J. Am. Chem. Soc.* **2005**, *127*, 6752–6765.
(20) Lenz, P.; Ajo-Franklin, C. M.; Boxer, S. G. *Langmuir* **2004**, *20*, 11092–11099.
(21) Saurel, O.; Cezanne, L.; Milon, A.; Tocanne, J. F.; Demange, P. *Biochemistry* **1998**, *37*, 1403–1410.
(22) Lin, W. C.; Blanchette, C. D.; Ratto, T. V.; Longo, M. L. *Biophys. J.* **2006**, *90*, 228–237.
(23) Boon, J. M.; Smith, B. D. *Med. Res. Rev.* **2002**, *22*, 251–281.
(24) John, K.; Schreiber, S.; Kubelt, J.; Herrmann, A.; Muller, P. *Biophys. J.* **2002**, *83*, 3315–3323.
(25) Groves, J. T.; Boxer, S. G. *Biophys. J.* **1995**, *69*, 1972–1975.
(26) Bard, A. J.; Fox, M. A. *Acc. Chem. Res.* **1995**, *28*, 141–145.

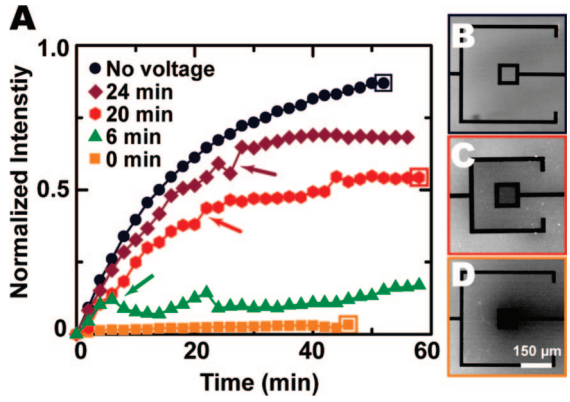

Figure 2. Temporal switching of lipid diffusion. Lipid conjugated fluorescent probes (Texas Red-DHPE) within the inner electrode were photobleached and allowed to recover for various times. (A) Arrows indicate the application of a 5 V amplitude, 1 kHz unipolar electric field for 1.5 min; time points are displayed in the legend. One sample was not exposed to an electric signal and served as the control (labeled no voltage). The data points were taken at 2 min intervals. Fluorescent intensity was background subtracted and then normalized. (B−D) Final states from the plots in (A) labeled no voltage, 20 min, and 0 min, respectively.

diffusion, determined by FRAP, required a ≥5 V field for 1 min. From 3 to 5 V, recovery was slowed, and below 3 V the recovery profile was unaltered (i.e., the recovery traces were indistinguishable from the water trace in Figure 1F).

To illustrate the temporal nature of diffusive gating, fluorescence recovery was electrochemically terminated at various time points (Figure 2). In this experiment, fluorophores within the middle square were photobleached, and the fluorescence intensity was monitored at 2 min intervals. An electric pulse (amplitude = 5 V, frequency = 1 kHz, duration = 1.5 min) was applied after 6, 20, and 24 min of unrestricted recovery. One sample was not exposed to an electric signal and served as the control, while another device was exposed to the field before photobleaching. The resulting traces were labeled "no voltage" and "0 min", respectively.

The absolute mechanism for electric gating of membrane diffusion was unclear; however, two explanations were considered. Prior work has established that alkanethiol monolayers electrochemically desorb from gold surfaces by application of sufficiently large electric fields.[28–30] Additionally, in the previous experiments, lipid gating was often accompanied by visible erosion of the metal layer. This affect was attributed to electrochemical dissolution of the metallic film into the aqueous phase. While either of these events could account for our observations, the relative time scales were not characterized. Therefore, the root cause of electrochemical lipid gating was not determined.

Passive Probe Reorganization. Under lower magnitude DC, fields the charged lipid probes were expected to organize into concentration gradients according to the relevant electrophoretic forces. In order to visualize probe reorganization, the bulk glass supported bilayer (region 1 as shown in Figure 3A) was segregated from the gold films by fibronectin barriers. Within the fibronectin barriers, two distinct phospholipid populations coexisted: a lipid bilayer over glass and a lipid monolayer over the alkanethiol/

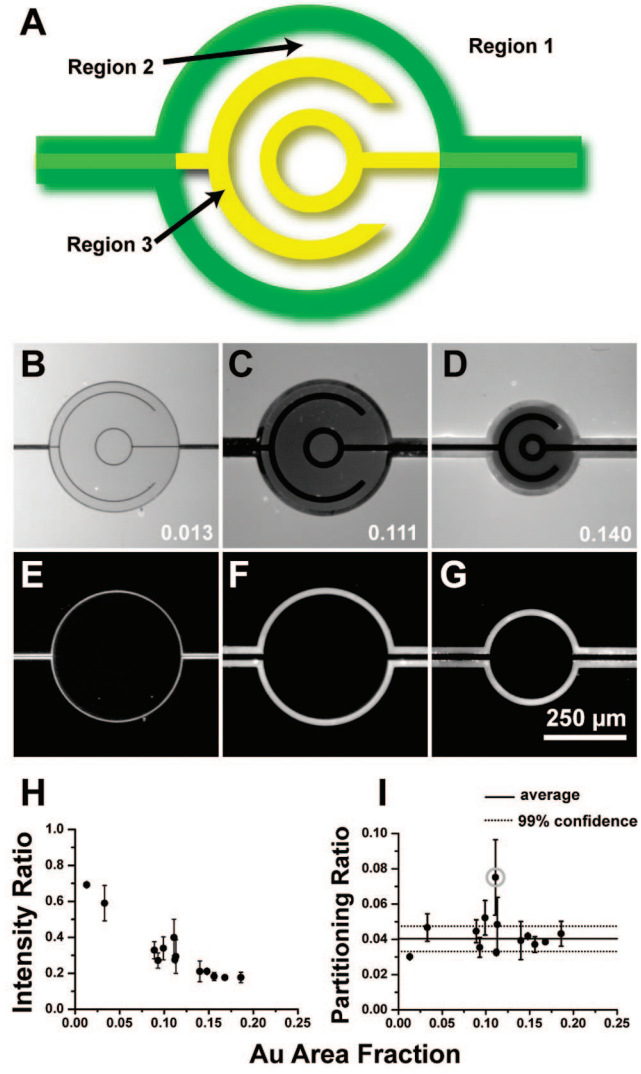

Figure 3. (A) Schematic of a second device design. The gold electrodes were enclosed within fibronectin barriers. Region 1 consisted of a uniform glass supported bilayer. Region 2 consisted of a glass supported bilayer in contact with an alkylated gold surface, region 3. (B−D) Equilibrium distribution of Texas Red-DHPE. Gold area fractions are indicated in the lower right corner. (E−G) Corresponding images of Alexa488 modified fibronectin. (H) Intensity ratio of region 2 over region 1 at various gold area fractions. (I) Partitioning ratio for the measured area fractions. The solid line represents the average partitioning ratio, 0.041, and the dotted lines correspond to a 99% confidence interval and represent 17% of the mean. The circled data point was determined to be a statistical outlier based on the *Q* test and was not included in the calculation of the mean.

gold surface (regions 2 and 3 as shown in Figure 3A). The segregation of these distinct membrane populations resulted in gradual reorganization of probe molecules, ultimately resulting in significantly less fluorescence intensity in region 2 compared to region 1. The most likely driving force for this redistribution of probe density was a difference in surface potential between the glass and alkanethiol/gold surfaces.

To verify this hypothesis, several different device geometries with unique gold area fractions were produced (Figure 3B−G). As expected, the increased gold area fraction resulted in a decreased intensity ratio between regions 1 and 2, indicating that more probes were accumulating over the gold surface (Figure 3H). Poisson–Boltzmann theory predicted that the ratio in probe densities, or partitioning ratio, between regions 2 and 3 was related to the difference in surface potentials and therefore independent of the relative area fractions of gold to glass.

(27) Moulton, S. E.; Barisci, J. N.; Bath, A.; Stella, R.; Wallace, G. G. *J. Colloid Interface Sci.* **2003**, *261*, 312–319.
(28) Walczak, M. M.; Popenoe, D. D.; Deinhammer, R. S.; Lamp, B. D.; Chung, C.; Porter, M. D. *Langmuir* **1991**, *7*, 2687–2693.
(29) Widrig, C. A.; Chung, C.; Porter, M. D. *J. Electroanal. Chem.* **1991**, *310*, 335–359.
(30) Zhang, Y.; Salaita, K.; Lim, J.-H.; Mirkin, C. A. *Nano Lett.* **2002**, *2*, 1389–1392.

In order to calculate the partitioning ratio, estimates of the probe density over the glass and gold surfaces were necessary.[31] In the limit of low fluorophore density, where self-quenching was minimal,[32] fluorescence intensity was linearly proportional to probe density. However, fluorescence intensity measurements of probes over the alkanethiol/gold surface were not possible for two reasons: fluorophore quenching by the metallic surface[16–18] and disruption of the light path (excitation and emission) by the metal layer on the inverted microscope. For these reasons, the probe density over the metallic surface was inferred through a series of assumptions: (1) all lipid leaflet densities, bilayer and monolayer, were equivalent, (2) the fluorescence intensity was linearly proportional to the probe density, (3) the probe density in region 1 was equivalent to that of the vesicles used for bilayer deposition (1 mol %), and (4) directly following vesicle fusion, the probe density was equivalent in all regions. The second assumption was necessary because the ratio of fluorescence intensities (designated F) between regions 2 and 1 provided a conversion factor (designated R_{conv}) to relate probe densities (designated ρ) in regions 1 and 2:

$$R_{conv} = \frac{F_{region2}}{F_{region1}} = \frac{\rho_{region2}}{\rho_{region1}} \quad (1)$$

Application of the third assumption resulted in an expression to determine the probe density in region 2:

$$\rho_{region2} = (R_{conv})(\rho_{vesicle}) \quad (2)$$

where $\rho_{vesicle}$ was kept constant at 1% mol fraction. The final assumption provided a mechanism to determine the total number of probe molecules within the area enclosed by the protein barriers (designated N_{device}) directly following vesicle fusion:

$$N_{device} = \rho_{vesicle} a_{region2} + \left(\frac{\rho_{vesicle}}{2}\right) a_{region3} \quad (3)$$

where a represents area and the factor of 2 takes into account that there was only a lipid monolayer over region 3. Following vesicle fusion, the charged probes began to redistribute according to the relevant surface potentials. The protein barriers blocked lipid diffusion, resulting in a gradual decrease in fluorescence intensity in region 2 compared to region 1, indicating that lipid probes were accumulating over the gold surfaces. At equilibrium (>1 h), when there was no longer a change in the relative intensities, R_{conv} was measured. This value was used to determine $\rho_{region2}$ via eq 2. The presence of the protein barriers ensured that the total number of probe molecules remained constant throughout the reorganization process, thereby providing a means to infer the probe density in region 3 at equilibrium:

$$\rho_{region3} = \frac{N_{device} - \rho_{region2} a_{region2}}{a_{region3}} \quad (4)$$

The ratio of probe densities between the two connected membranes, or partitioning ratio (designated f), offered a route to determine the difference in surface potentials between the glass and alkylated gold surfaces, $\Delta\Psi$, via the Boltzmann-weighted difference in the electrostatic energy of a probe in region 2 and region 3,[31]

$$f = \exp[-ze(\Psi_{region3} - \Psi_{region2})/k_B T] \quad (5)$$

were k_B is Boltzmann's constant, T is absolute temperature, e is the elementary charge, and z is the probe charge. An average partitioning ratio was calculated from 12 unique devices at room temperature with varying area fractions of gold. As expected from Poisson–Boltzmann theory, a plot of the partitioning ratio versus gold area fraction resulted in a flat distribution (Figure 3I). From these experiments, the mean partitioning ratio was found to be 0.041 ± 0.007 (99% confidence). This implies a surface potential difference of 80 ± 10 mV, and it provided an explanation for the decreased fluorescence intensity within the protein enclosure.

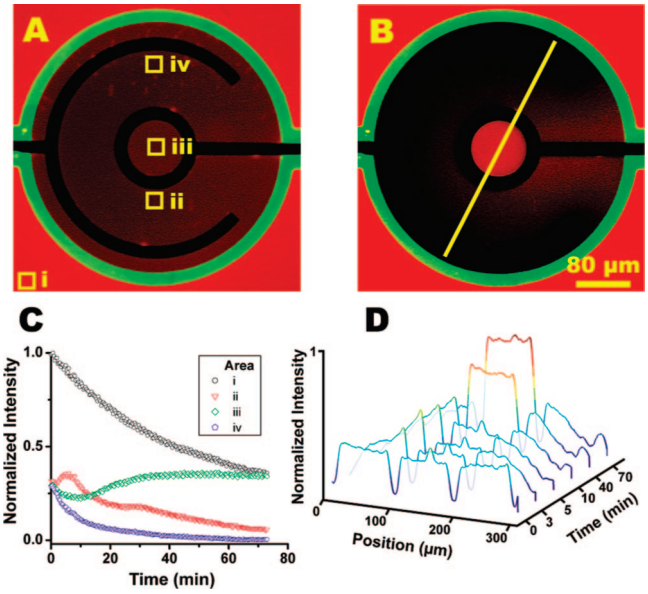

Figure 4. Two dimensional electrophoresis of negatively charged lipid probes. (A) Initial state of the lipid membrane before application of an electric potential. (B) Probe distribution after application of 1.5 V for 70 min. The contrast in images A and B was digitally adjusted (in Adobe Photoshop) for facile comparison. (C) Time traces of normalized probe intensity from locations indicated in (A). (D) Normalized fluorescence intensity line scans indicated in (B).

Induced Reorganization. With this understanding of the passive surface potential driven reorganization of charged lipid probes, we investigated active reorganization by application of DC fields too small to promote thiol desorption. Fluorescence intensities were monitored at four positions (areas i, ii, iii, and iv indicated in Figure 4A) before and after application of a 1.5 V potential difference. At $t = 0$, before application of the potential, the fluorescence intensity in region 2 (as defined in Figure 3A) was approximately 30% of that in region 1. The uniformity in fluorescence intensity across areas ii−iv indicated equilibrium. Initially, (<15 min) following application of the electric potential, the charged probes began to reorganize according to the relevant electrophoretic forces. Probe molecules were repelled from the outer negative electrode, manifested by a sharp decrease in intensity (Figure 4C, area iv trace). Simultaneously, probes were attracted toward the positive center electrode which resulted in decreased intensity within the inner electrode (Figure 4C, area iii trace) and increased intensity near the electrode as probes moved through that area to accumulate over the positive electrode (Figure 4C, area ii trace).

Over time (>15 min), the probe density increased over the inner electrode surface and probes began to spill over into the inner electrode where there was no apparent electric field, resulting in significant increases in probe density within area iii. Continued accumulation of probe density over the inner electrode resulted in the delayed decrease in intensity within area ii. This accumulation process was also visualized by a series of line scans (Figure 4D). The accumulation was reversible by switching

(31) Parthasarathy, R.; Cripe, P. A.; Groves, J. T. *Phys. Rev. Lett.* **2005**, *95*, 048101.

(32) Macdonald, R. I. *J. Biol. Chem.* **1990**, *265*, 13533–13539.

the polarity (see the Supporting Information).

The probe intensity within the bulk membrane (area i) was monitored to determine the intrinsic photobleaching rate (Figure 4C, area i trace). Although the membrane in this area was connected to a nearly infinite lipid supply, due to the large field of view (nearly 1 mm^2), the replenishment rate into area i was severely limited by diffusion across > 300 μm to the illumination edge. This was confirmed by the spatially flat intensity profile from area i to the illumination edge over the 70 min time frame (data not shown). However, the other traces in Figure 4C were not normalized by the area i trace because of an apparent difference in bleaching rates between regions 1 and 2. As probes accumulated over the gold electrodes, they were blocked from the excitation illumination. These fluorophores were not bleached but were free to diffuse into the illumination area at a later time, thereby reducing the observed bleaching rate. However, bleaching did occur within region 2; therefore, the flat portion of the area iii trace is misleading: probe molecules continued to accumulate within this region after 60 min.

To demonstrate the utility of this device as a potential cell mimic, His-10 modified GFP was conjugated to the membrane surface by attachment to Ni^{2+}-NTA-DOGS lipids.[33] Prior work has established that proteins coupled to supported membranes move by electro-osmosis,[34] thus offering an additional route to image the forces at play within this device. DC fields, of the same polarity as previously discussed, resulted in the accumulation of protein near the outer electrode surface (Figure 5B). In this experiment, low fibronectin density provided ineffective barriers to lipid and protein motion. Reversal of the electric field resulted in collective protein motion toward the opposite electrode, resulting in accumulation of protein within the inner electrode (Figure 5C and D), reminiscent of formation of the immunological synapse.[35] As time passed, proteins were pumped out of the inner electrode until the distribution settled toward a steady state density profile (Figure 5D–F).

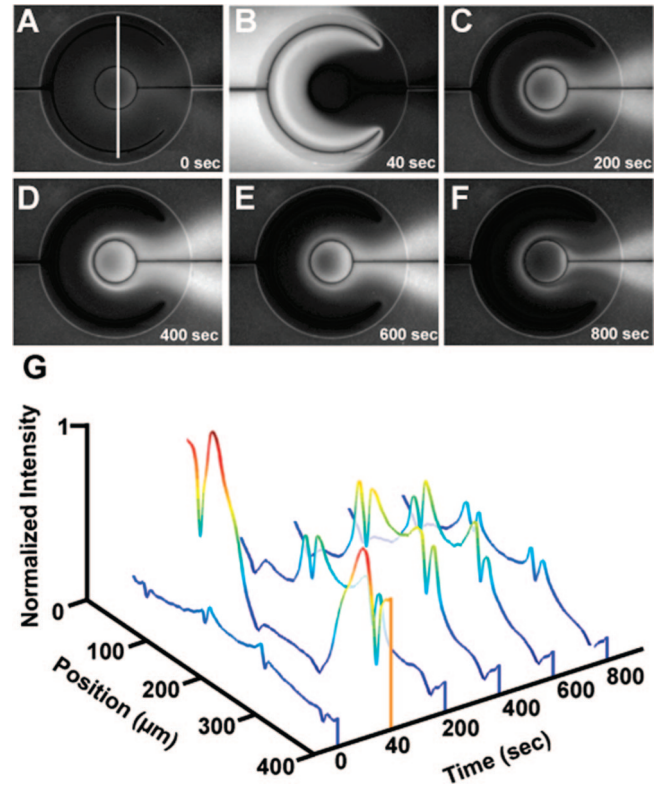

Figure 5. Electro-osmotic manipulation of GFP His-10. (A) Initial state before exposure to (B) 2.0 V potential difference then (C) reversal of polarity to –2.0 V and (D−F) subsequent relaxation to a steady state distribution at this voltage. (G) Normalized fluorescence intensity line scans indicated in (A).

Conclusions

Many cellular processes are known to be dynamic. Supported membranes, as two-dimensional fluids, allow for dynamic rearrangement of biological species. However, few studies have attempted to control membrane components at biologically relevant time scales. Electrical switching of membrane diffusion represents the only technique capable of gating lipid motion at time scales comparable to T-cell synapse formation (<5 min). Two-dimensional electrophoretic and electro-osmotic manipulation of charged lipids and membrane associated proteins, respectively, provided a reversible means to accumulate biomolecules into unique distribution profiles.

Acknowledgment. This work was supported by the Chemical Sciences, Geosciences and Biosciences Division, Office of Basic Energy Sciences, of the U.S. Department of Energy under Contract No. DE-AC03-76SF00098 and NIH training Grant GM08295 to B.L.J. All devices were made in the UC Berkeley Microlab. We thank Cheng-Han Yu for his advice with optical lithography, Nathan Clack for his assistance with MatLab, and William Galush and Khalid Salaita for helpful discussions.

Supporting Information Available: Movies of fluorescence images and the corresponding intensity line scans illustrating the reorganization process. This material is available free of charge via the Internet at http://pubs.acs.org.

LA800040W

(33) Nye, J. A.; Groves, J. T. *Langmuir* **2008**, *24* (8), 4145−4149.
(34) Groves, J. T.; Wulfing, C.; Boxer, S. G. *Biophys. J.* **1996**, *71*, 2716–2723.
(35) Monks, C. R. F.; Freiberg, B. A.; Kupfer, H.; Sciaky, N.; Kupfer, A. *Nature* **1998**, *395*, 82–86.